Available online at www.sciencedirect.com
SCIENCE DIRECT
Polymer 47 (2006) 728–734
polymer
www.elsevier.com/locate/polymer

One-step synthesis of dextran-based stable nanoparticles assisted by self-assembly

Minhua Tang, Hongjing Dou, Kang Sun *

State Key Lab of Metal Matrix Composites, Shanghai Jiao Tong University, 1954 Huashan Road, Shanghai 200030, China

Received 22 June 2005; received in revised form 17 October 2005; accepted 30 November 2005
Available online 20 December 2005

Abstract

We present a facile method to prepare stabilized nanoparticles with pH-sensitivity and controllable dimension directly from dextran and two kinds of monomers. The synthesis was realized by a self-assembly assisted graft copolymerization of AA from dextran under the presence of crosslinker—*N*,*N*′-methylene bisacrylamide. This approach was characterized as organic solvent free, surfactant free and comparatively high solid contents (~40 mg/ml). The polymerization of AA was confirmed by FT-IR, and TGA analysis. The resultant nanoparticles were studied by TEM, AFM, SEM, DLS and zeta-potential measurements. It was found that the size of resultant dextran-based nanoparticles ranges from 40 to 140 nm, and depends greatly on R_{GM} [(glucose unit)/AA (mol:mol)] during polymerization. Besides, the nanoparticles have obvious pH-sensitivity because of the presence of carboxy groups in the nanoparticles.

Keywords: Nanoparticles; Dextran; Self-assembly

1. Introduction

For applications in numerous fields such as nucleating agent [1], nanoreactors [2], drug delivery [3] etc., nanoparticles have attracted a rapidly growing interest [4]. In the past decades, more and more attention was paid to fundamental studies and technological developments of polymeric nanoparticles [5]. A conventional way to produce polymeric nanoparticles was emulsion polymerization [6–8], but some drawbacks, such as complicated processing for removing surplus surfactant and purifying resultant nanoparticles, limited the applications of this method in some fields. In recent years, self-assembly approach had developed to be an efficient approach to fabricate nanoparticles from amphiphilic copolymers. For example, Wooley's group synthesized stable nanoparticles with core-shell morphology by the self-assembly of diblock copolymers and succedent crosslinking of the 'shell' part [9]. Furthermore, Armes et al. made great progress in fabricating crosslinked nanoparticles at high solid content by using ABC tri-block copolymers in the fabrication of core-shell-corona nanoparticles, which allowing inner-shell cross-linking to be carried out at high solids (<10 w/v%) without any interparticle cross-linking [10].

Polysaccharides, due to their unique physicochemical properties and excellent biocompatibility, should be appropriate to prepare nanoparticles applicable in many fields, especially for biomedical purpose. However, there are only a few reports about fabricating nanoparticles from polysaccharides. For example, M. Jiang et al. synthesized one kind of hydroxyethyl cellulose (HEC)-based nanoparticles, which characterized with a pH-sensitive morphological transition from core-shell micelles to hollow spheres [11]. Hu et al. synthesized chitosan-poly(acrylic acid) nanoparticles by template polymerization, the nanoparticles were made of completely hydrophilic polymers without using any organic solvents and surfactants [12]. But in this method, the driving force of the formation of nanoparticles is the electrostatic interaction between amino groups of chitosan and carboxylic groups of PAA, which limited the applicability of this method to other polysaccharides, which are nonionic.

Dextran, one kind of water-soluble polysaccharide, is produced industrially in a large scale and has wide application in food and medical fields [13]. Herein, aimed at improving the practicability of polymeric nanoparticles, we chose dextran combined two kinds of monomer to synthesize nanoparticles directly. Our work are characterized with the features as follows: (1) the synthesis includes only one step and the resultant aqueous solutions of nanoparticles have relatively

* Corresponding author. Tel.: +86 21 629 32555; fax: +86 21 628 30735.
E-mail address: ksun@sjtu.edu.cn (K. Sun).

0032-3861/$ - see front matter © 2005 Elsevier Ltd. All rights reserved.
doi:10.1016/j.polymer.2005.11.091

high solid contents (~40 mg/ml); (2) the nanoparticles are synthesized in a completely aqueous solution without any organic solvent and surfactant; (3) the nanoparticles have controllable nano-sized dimension and obviously pH sensitivity, the carboxyl groups in the resultant nanoparticles made them promising in loading cationic targets.

2. Experimental section

2.1. Materials

Dextran (Sinopharm Chemical Reagent Co. Ltd, China, M_w=20,000) was used directly. Acrylic acid (Sinopharm Chemical Reagent Co. Ltd, China) was dried by $MgSO_4$ and then vacuum distilled before use. *N*,*N*′-Methylene bisacrylamide (MBA) (Fluka) was re-crystallized from methanol. Cerium (IV) ammonium nitrate (CAN) (Sinopharm Chemical Reagent Co. Ltd, China) was re-crystallized from dilute nitric acid (Sinopharm Chemical Reagent Co. Ltd, China) containing appropriate ammonium nitrate (Sinopharm Chemical Reagent Co. Ltd, China).

2.2. Synthesis of dextran-based nanoparticles

Cerium (IV) was used as an initiator for the graft copolymerization of various monomers from dextran or other hydroxyl group containing macromolecules [14]. When ceric ions are added in the reaction mixture for grafting on dextran, a ceric ion–dextran complex is initially formed which immediately creates a free radical at the backbone of the dextran and ceric ions are reduced to cerous ions through an one-electron transfer process. The reactivity of the ceric ions is pH-dependent; hence, during grafting, the concentration of the nitric acid was maintained at ca. 0.002 mol/L and the pH of the solution is kept around 2.

The dextran-based nanoparticles were synthesized by the process as follows: 2.5 mg dextran was dissolved in 50 ml deionized water at 25 °C under gentle stirring and nitrogen bubbling, then the solution of a designated amount of CAN in 1.25 ml 0.1 N nitric acid and a designated amount of AA were successively added. Twenty minutes later, MBA was added and the reaction was kept at 30 °C for 4 h. Thereafter, 1 M NaOH was added to neutralize the reaction system. Finally, the reaction solution was dialyzed against deionized water for 3 days using the membrane bag with a 14,000 cut-off molecular weight to remove the un-reacted monomers and the un-grafted PAA. The final aqueous solutions were lyophilized to get solid nanoparticles.

Table 1
The ratios of reagents in the synthesis of dextran–PAA nanoparticles

Sample no.	GU (glucose unit):AA (acrylic acid), mol:mol (R_{GM})	AA:initiator, mol:mol (R_{MI})	AA:crosslinkor (MBA), mol:mol (R_{MC})
NP1a	1	7	10
NP1.5	1.5	7	10
NP2	2	7	10
NP3	3	7	10
NP4	4	7	10
NP1b	1	10	10
NP1c	1	14	10

Table 2
The ratio of reagents in the synthesis of dextran–PNIPAM

Sample no.	GU (glucose unit):NIPAM, mol:mol (R_{GN})	NIPAM:initiator, mol:mol (R_{NI})	NIPAM:crosslinkor (MBA), mol:mol (R_{NC})
NPN	2	7	10

For investigating the influence of the ratio of reagents on the resultant nanopariticles, several kinds of nanoparticles were synthesized under different ratios of reagents (as shown in Table 1).

In order to explore the mechanism of this one-step synthesis and investigate the importance of the complexation of PAA and dextran during synthesis, *N*-isopropylacrylamide (NIPAM) was chosen as a substitute of AA in the synthesis of dextran-based nanoparticles. NIPAM is also a monomer but has not complexation with dextran [15]. The ratio of reagents is listed in Table 2.

2.3. Yield of the synthesis and the composition of NP1a and NP2

The yield in the synthesis of nanoparticles and the composition of NP1a and NP2 are calculated as follows:

$$\text{Yield} = \frac{W_s}{W_t} \times 100\%$$

$$\text{Dextran\% in the nanoparticles} = \frac{W_D}{W_S} \times 100\%$$

(PAA and MBA)% in the nanoparticles

= 1 − (dextran% in the nanoparticles)

W_s: the weight of resultant nanoparticles after freeze–dry; W_t: the total weight of the reagents during synthesis; W_D: the weight of dextran used in the synthesis.

We synthesized several kinds of nanoparticles under different ratios of reagents. The yield in the synthesis of each sample was listed in Table 3.

2.4. FT-IR spectrum analysis

FT-IR spectra of the samples in their aqueous solutions were measured by a Bruker EQUINOX 55 spectrometer to analyze the composition of resultant nanoparticles.

Table 3
The yield in the synthesis of each sample

Sample no.	NP1a	NP1.5	NP2	NP3	NP4	NP1b	NP1c
Yield (%)	79.0	77.8	73.1	75.4	64.5	65.2	56.1

2.5. TGA analysis

The TGA analysis of NP1a, NP2, dextran ($M_W = 20{,}000$) and PAA ($M_W = 2000$, Aldrich) was conducted by TGA 2050, (TA Co. Ltd) at a heat rate of 20 °C/min under nitrogen atmosphere.

2.6. Hydrodynamic diameter of dextran–PAA nanoparticles

The hydrodynamic diameter of the resultant nanoparticles was measured by dynamic light scattering (DLS) (Malvern Autosizer 4700). For investigating the pH-sensitivity of nanoparticles, the nanoparticles were dissolved in the buffers at different pH values to keep the pH constant during measurement. All DLS measurements were done with a wavelength of 532 nm at 25 ± 0.1 °C and a fixed scattering angle of 90°.

2.7. Zeta-potential of dextran–PAA nanoparticles

The zeta-potential of resultant nanoparticles was measured by Malvern Zetasizer 2000. For investigating the pH-sensitivity of nanoparticles, the nanoparticles were dissolved in the buffers at different pH values to keep the pH constant during measurement. Each sample was repeatedly measured five times and the values reported were the average values.

2.8. Atomic force microscopy (AFM)

Atomic force microscopy (AFM) (SEKO SPI 3800N Probe Station) was used to observe the morphology of the resultant nanoparticles. Samples were dropped onto new-cleaved mica slices and dried at room temperature for at least 72 h.

2.9. Transmission electron microscopy (TEM)

Transmission electron microscopy (TEM) (PHILIPS CM 120 BioTwin) was also used to observe the morphology of the resultant nanoparticles. The samples were negative stained by using phosphotungstic acid and placed onto carbon-coated copper grid followed by drying at room temperature for at least 72 h.

2.10. Scan electron microscopy (SEM)

Scan electron microscopy (SEM) (SIRION 200, PHILIPS) was also used to observe the morphology of the resultant nanoparticles. The samples were place on a copper substrate and dried at room temperature before gold sputtering.

3. Results and discussion

3.1. Size, morphology and mechanism

Dynamic light scattering (DLS) can effectively characterize the nanoparticles in solution, therefore, the dimension of resultant nanoparticles were characterized firstly by DLS. DLS measurements reveal that NP1a nanoparticles have an average hydrodynamic diameter $\langle D_h \rangle$ of 130 nm and the distribution of $\langle D_h \rangle$ was shown in the insert of Fig. 1(a).

The morphology of resultant nanoparticles was observed by TEM, SEM and AFM. Phosphotungstic acid was used as a negative stained reagent to facilitate TEM observation [16], and the negative stained TEM images of NP1a and NP2 are shown in Fig. 1. Both two samples demonstrate spherical morphology with a dimension of 50–100 nm. Besides, SEM and AFM are both powerful instruments to observe the three-dimensional morphology of nanoparticles. Fig. 2 shows the SEM and AFM (as insert) microimages of NP1a and NP2, it is

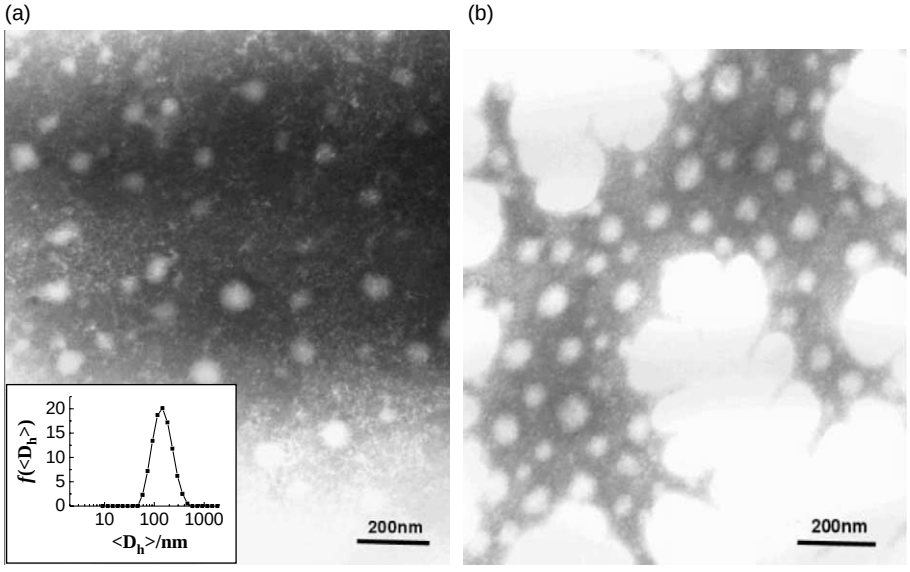

Fig. 1. The negative stained TEM images of (a) NP1a and (b) NP2. The insert is the distribution of D_h of NP1a.

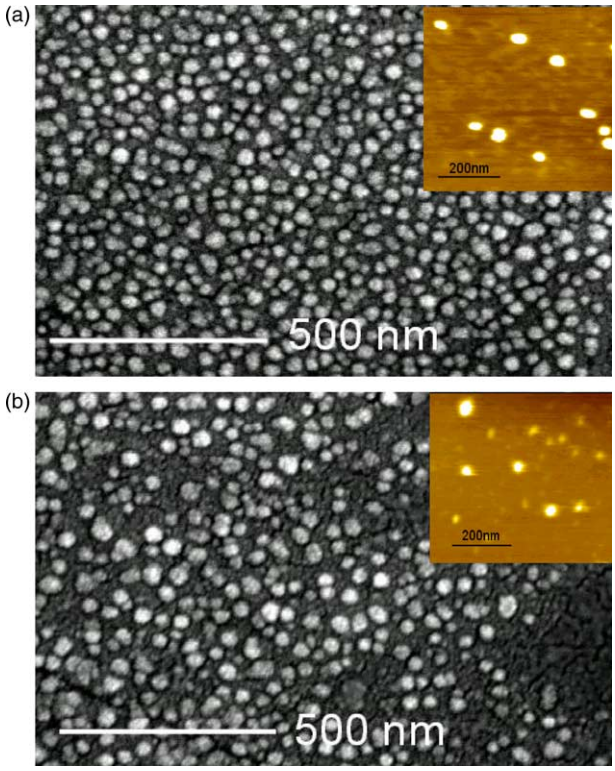

Fig. 2. The SEM images of (a) NP1a and (b) NP2. The inserts are AFM images, the vertical scale is 5 nm (from dark to bright).

obvious that both these two kinds of nanoparticle had the dimension of around 50 nm and the average size of NP1a is a little larger than that of NP2.

Generally speaking, the polymerization of AA with MBA acting as corss-linker results in hydrogel [17,18]. However, TEM, SEM and AFM observation confirmed that nanoparticles instead of macro-hydrogel formed at the presence of dextran in our experiment. From the results, it is reasonable to conclude that the presence of dextran should play a crucial role in our one-pot synthesis to nanoparticles. Both dextran and PAA are water-soluble macromolecules, and it has been confirmed [11,15] that many hydrophilic polysaccharides, including dextran, can form interpolymer complexes (IPC) with PAA in acid medium owing to hydrogen bond interaction of carboxyl groups and proton-acceptors in glucose units. Thus, the hydrophobic driving force for the formation of nanoparticles should be attributed to the complexation of PAA grafts and dextran segments. To validate the effect of the PAA–dextran complexation on the fabrication of nanoparticles, we chose another monomer—*N*-isopropylacrylamide (NIPAM), which cannot form complex with dextran backbone at acidic medium [15], to participate in the polymerization as a substitute of AA in the synthesis of NP2. DLS results disclosed a $\langle D_h \rangle$ of 36.6 nm of resultant product, which is comparable to the $\langle D_h \rangle$ of dextran macromolecular chains determined by DLS, and excluded the formation of nano-aggregates, whereas a control experiment using AA as monomer (NP2 nanoparticles) demonstrated the formation of the nanoparticles with a average diameter of 103 nm. Therefore, the complexation of the grafts and the main chains is indispensable in the proposed approach to get dextran-based nanoparticles. We propose the mechanism of this process is as follows (as shown in Scheme 1): after initiation of graft copolymerization of AA from dextran, the PAA grafts will complex with dextran due to hydrogen bond interaction and as a result, the self-assembly occurs and the 'micelle'-like nano-aggregates forms. As no macroscopic precipitation takes place in this process, we suggest that the dextran chains with less complexed segments may still keep solvated and thus stabilize the complex aggregates. This self-assembly assisted process has been verified crucial to the formation of nanoparticles by the control experiment of taking NIPAM as a substitute of AA. Subsequently, participation of bifunctional monomer—MBA in the copolymerization leads to

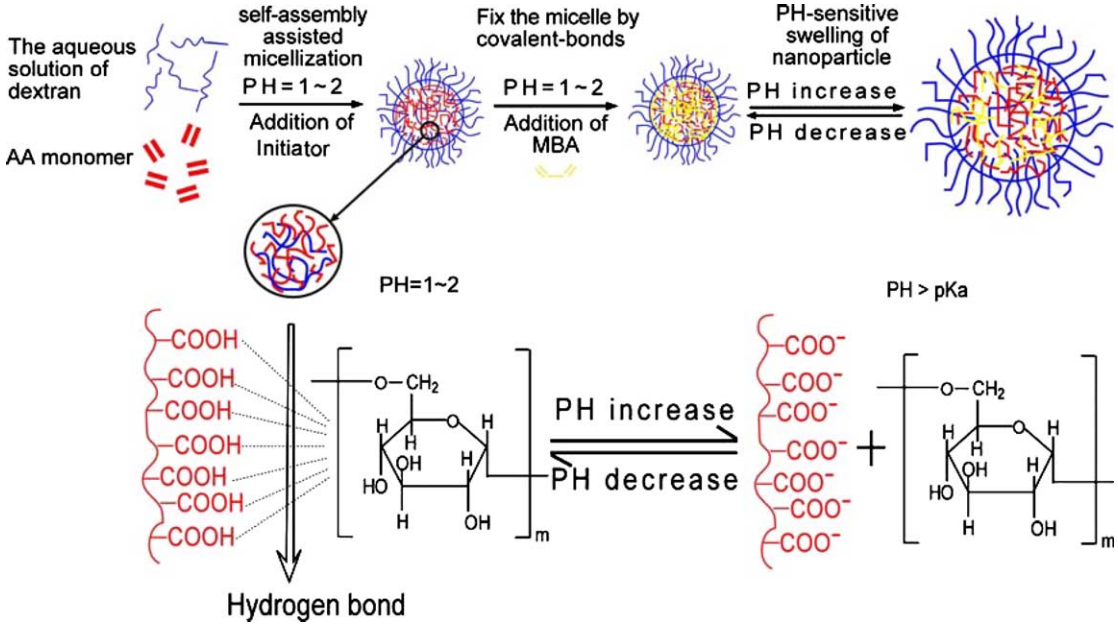

Scheme 1. The synthesized mechanism of dextran-based nanoparticles.

the further fixation of the structure by crosslinking the PAA chains using covalent bonds. Thanks to the shielding effect of the dextran segments in periphery, the inter-particle cross-linking is prevented. The stability of the nanoparticles is confirmed by the fact that they still hold the integral structure at pH 7 in which the hydrogen bond between dextran and PAA has been destroyed because of the deprotonation of carboxyl groups in PAA [15].

3.2. Composition of the nanoparticles

Fig. 3 shows the FT-IR spectra of PAA (a), dextran (b) and NP1a at neutral medium (c). Compared with pure dextran, two new absorption peaks of NP1a nanoparticles at 1539 and 1419 cm^{-1} could be assigned to asymmetric and symmetric stretching vibrations of COO^- groups, the absence of –COOH absorption peaks is due to most carboxyl groups exists in the form of $–COO^-$ at neutral medium (the p*K*a of PAA is around 4.75 [19]). The peak at 2924 cm^{-1} is the absorption of the CH_2 groups in PAA grafts. Furthermore, the band at 1000–1100 cm^{-1} typical for ether linkages of dextran could also be found in the spectrum of NP1a nanoparticles. By FT-IR measurements, the main compositions of NP1a nanoparticles were confirmed as dextran and PAA.

Furthermore, the TGA analysis gives additional information about the composition of the resultant nanoparticles. The thermograms of PAA, dextran, NP1a and NP2 are shown in Fig. 4. The thermogram of dextran (Fig. 4(a)) exhibits two decomposition stages. The first one (below 130 °C) is due to the loss of water, and the other in the range of 250–350 °C has been described to the degradation of saccharide structure [20]. The thermogram of PAA shows three decomposition stages. The first decomposition stage in the range of 50–130 °C is attributed to the loss of bound water. The second one in the interval of 150–330 °C has been described to the dehydration and decarboxylation of the polymer which leads to the formation of inter-and intra-molecular anhydride [20,21]. The third decomposition stage in the range of 330–500 °C is a result of the degradation of the residual polymer. Compare the

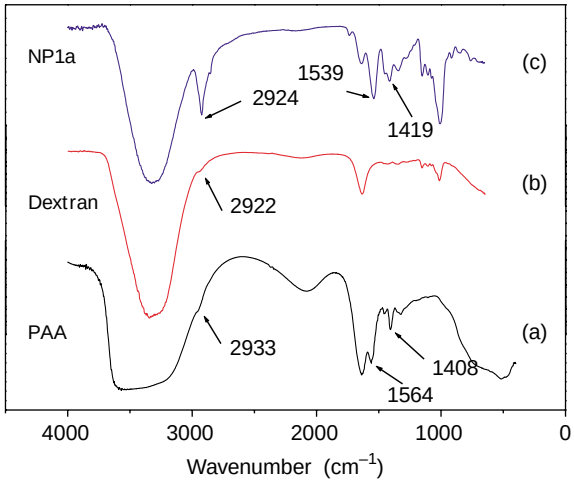

Fig. 3. The FT-IR spectra of PAA (a), dextran (b) and NP1a (c).

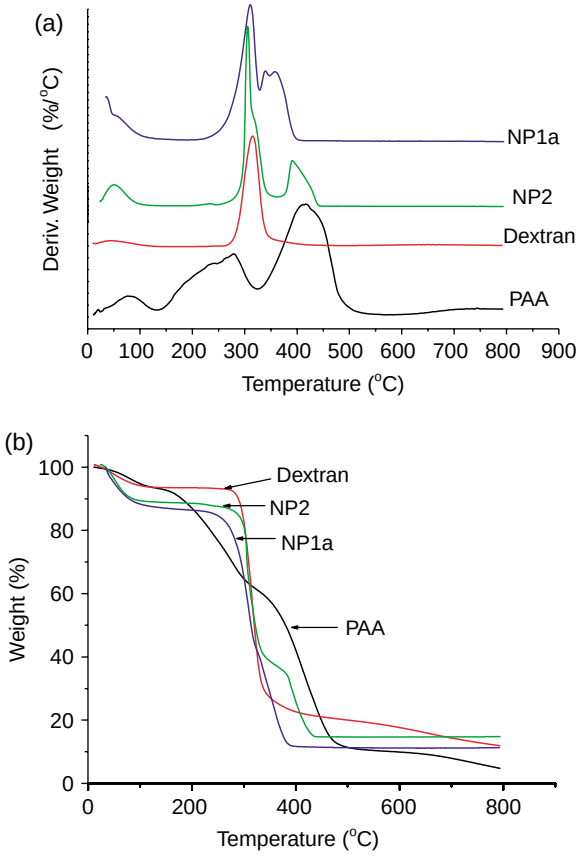

Fig. 4. The thermograms of PAA, dextran, NP1a and NP2.

thermograms of NP1a and NP2 with that of dextran, the new decomposition stage around 360 °C proves the presence of PAA in dextran-PAA nanoparticles. And the absence of decomposition stage in the range of 150–330 °C shows the dehydration and decarboxylation of PAA do not occur before PAA degrades. TGA analysis suggests that the state of carboxyl groups in resultant nanoparticles is different from that in pure PAA, there are interaction between carboxyl groups and dextran chains and this interaction increases the stability of PAA. Comparing the thermograms of NP1a with that of NP2, the third stage weight loss of NP1a (∼40%) are greater than that of NP2 (∼25%), suggested that there are more PAA in NP1a than NP2, this result is coherent with the composition of NP1a and NP2 calculated by the weight-calculated approach as explained in 2.3 (as shown in Table 4). Besides, compare with PAA, the third decomposition stage which was assigned to the degradation of PAA moves to lower temperature, and the decomposition temperature decreases according to the sequence of PAA, NP2 and NP1a.

Table 4
The composition of NP1a and NP2 calculated from the weight-calculated approach as explained in experimental section

Sample no.	NP1a	NP2
Dextran% in the samples	62.4	90.2
PAA and MBA% in the samples	37.6	9.8

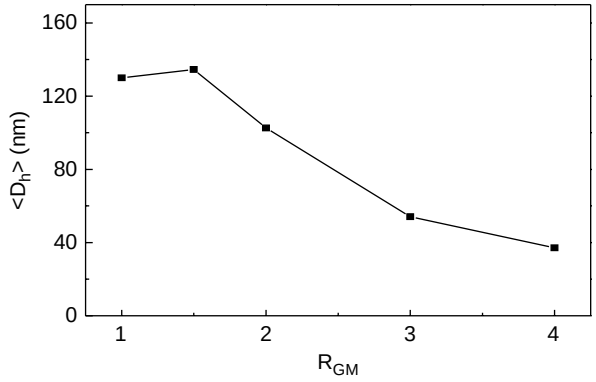

Fig. 5. The variation of $\langle D_h \rangle$ value with R_{GM} in water.

This suggests that the interaction between carboxyl groups and dextran chains increases with the amount of carboxyl groups.

3.3. Effect of R_{GM} and R_{MI} on the nanoparticles

Now that the key effect of the complexation between PAA and dextran in the synthesis has been verified, it is rational to speculate that the resultant nanoparticles will have significant dependence upon the content of PAA and dextran during synthesis, because the dextran–PAA complexation has great relationship with molar ratio of the repeated units of dextran and PAA (M_{GU}/M_{AA}) [15]. To investigate the effect of M_{GU}/M_{AA} (R_{GM}) on the resultant nanoparticles, we investigated $\langle D_h \rangle$ variation of the nanoparticles with the R_{GM} by DLS. The results are shown in Fig. 5. It is obvious that the decrease of AA content in synthetic process results in the decrease of the dimension of resultant nanoparticles, at the condition of keeping the contents of other reactants constant. That indicates fewer AA results in smaller nanoparticles in synthesis. Decreasing R_{GM} on the condition of keeping R_{MI} and R_{MC} constant, means decreasing the average number of PAA grafts with similar length in every dextran backbones, which will decrease the size of the hydrophobic complex of dextran and PAA, therefore, decrease the size of the nanoparticles derived from dextran–PAA complexation. Analogous phenomenon has been reported in the micellization of amphiphilic graft copolymers [22] and block copolymers [23].

The $\langle D_h \rangle$ of NP1a and NP2 obtained from DLS measurement are 130 and 103 nm, respectively, which are larger than diameters observed by TEM, SEM and AFM. That should be due to the shrinkage of nanoparticles during drying of the samples, similar shrinkage during sample preparation of microscopy observation has been reported in the research of other nanoparticles [24].

Table 5
The variation of zeta-potential with R_{GM} in water (under pH = 6.7)

Sample no.	R_{GM}	Zeta-potential (mV)
NP1a	1	−14.1
NP1.5	1.5	−11.0
NP2	2	−13
NP3	3	−7.7
NP4	4	−8.9

Table 6
The variation of $\langle D_h \rangle$ with R_{MI} in water

Sample no.	R_{MI}	$\langle D_h \rangle$ (nm)
NP1a	7	130
NP1b	10	100.7
NP1c	14	136.4

From the results of zeta-potential listed in Table 5, the zeta-potential of dextran–PAA nanoparticles in water are mostly around −10 mV. Besides, the variation of R_{GM} had almost no effect on zeta-potential of the nanoparticles. The zeta-potential values of NP2 and NP4 are only slightly more negative than NP1.5 and NP3, respectively (less than 2 mV), this aberrancy should be reasonable taking the instrument error into account (the normal instrument error of zeta-potential instrument is ±2 mV). The small numbers of zeta-potential indicate that in these dextran–PAA nanoparticles, most PAA chain are wrapped by dextran segments and mainly locate in the inner part of the nanoparticles.

We also investigated the variation of $\langle D_h \rangle$ with R_{MI} by DLS. The results are listed in Table 6. It is showed that the $\langle D_h \rangle$ has not remarkable variation with the change of R_{MI}, on the condition of keeping R_{GM} and R_{MC} constant. The zeta-potential analysis (Table 7) shows that with the increase of R_{MI} from 7 to 14, i.e. decreasing the amount of initiator, the zeta-potential of nanoparticles shift to negative direction. This result suggests that at bigger R_{MI}, there might be more PAA segments able to extend to the periphery of the nanoparticles.

3.4. pH-sensitivity of the nanoparticle

The variation of $\langle D_h \rangle$ and zeta-potential of NP1a and NP2 with the pH of mediums were studied by DLS and zeta-potential measurement. The aqueous solutions of nanoparticles at different pH values were obtained by dissolving nanoparticles in different buffers. The results are listed in Table 8.

It is found that the nanoparticles are remarkably sensitive to the pH of medium. The $\langle D_h \rangle$ of nanoparticles increase and the zeta-potential decrease with the increase of pH. The result could be rationalized by the mechanism we proposed about the formation of dextran-based nanoparticles. At pH 3.43, most carboxyl groups in PAA are protonated (because the p*K*a of PAA is 4.75 [19]) and the complexation between PAA and dextran renews again, which result into the shrinkage of nanoparticles. With the pH increasing to 6.69, most carboxy groups are exist in the form of $-COO^-$ due to their deprotonation, the complex of dextran and PAA is destroyed,

Table 7
The variation of zeta-potential with R_{MI} in water (under pH = 6.7)

Sample no.	R_{MI}	Zeta-potential (mV)
NP1a	7	−14.1
NP1b	10	−23.3
NP1c	14	−29.6

Table 8
The variation of $\langle D_h \rangle$ and zeta-potential with pH values

NP1a			NP2		
pH	$\langle D_h \rangle$	Zeta-potential	pH	$\langle D_h \rangle$	Zeta-potential
3.43	77.3	2.7	3.43	60.8	2.6
6.69	145.2	−14.1	6.69	79.2	−13
8.70	241.7	−17.2	8.94	144.4	−14.3

and the nanoparticles expend subsequently because of the electrostatic repulsion between $-COO^-$ groups. The zeta-potential at this pH changed to around −14. The decrease of zeta-potential is also the representation of the deprotonation of PAA. Furthermore, at pH 8.7, more carboxyl groups deprotonate and exist in the form of $-COO^-$, the further decomposition of dextran–PAA complex and the stronger electrostatic repulsion between $-COO^-$ lead to further increase of $\langle D_h \rangle$. The unconspicuous variation of zeta-potential with the further increase of pH should because of the shielding effect of the dextran segments in the periphery of nanoparticles to the negative charge inside the nanoparticles.

4. Conclusion

In summary, we have developed a facile self-assembly assisted approach to synthesize dextran-based nanoparticles. By the approach, the aqueous solution of dextran-based nanoparticles at high solid contents could be obtained directly from monomers without using any organic solvents and surfactant. Because the mechanism of the synthesis is based on the complexation of dextran and PAA in acidic medium, this approach is anticipated to be applicable to multifarious water-soluble polysaccharides, which have complexation with PAA. The resultant nanoparticles have stable structure and obviously pH-sensitivity. Besides, it is found that the size of nanoparticles dependent significantly on R_{GM}, but R_{MI} has little effect on the size and has great effect on the zeta-potential of the nanoparticles. In this one-step synthesis, the use of renewable material as the central material, as well as a benign solvent medium, offers this approach numerous benefits ranging from environmental safety to applications in biologically relevant systems.

Acknowledgements

Financial support from Young Scholar's foundation of Shanghai Jiao Tong University and science and Technology Committee of Shanghai (Project No 05ZR 14084 and Project No 04DZ 14002) is gratefully acknowledged. Prof M. Jiang of Fudan University is thanked for his kind assistance of DLS studies. Instrumental Analysis Center of Shanghai Jiao Tong University is thanked for the assistance of FT-IR analysis.

References

[1] Tang J, Wang Y, Liu H, Belflore LA. Polymer 2004;45:2081–91.
[2] Rutnakornpituk M, Thompson MS, Harris LS, Farmer KE, Esker AR, Riffle JS, et al. Polymer 2002;43:2337–48.
[3] Liu SY, Weaver VMJ, Save M, Armes SP. Langmuir 2002;18:8350–7.
[4] (a) Botha SS, Brijoux W, Brinkmann R, Feyer M, Hofstadt HW, Kelashvili G, et al. Appl Organomet Chem 2004;18:566–72.
(b) Pellegrino T, Kudera S, Liedl T, Javier AM, Manna L, Parak WJ. Small 2005;1:48–63.
(c) Hedden RC, Bauer BJ, Smith AP, Grvhn F, Amis E. Polymer 2002; 43:5473–81.
[5] (a) Zhang L, Eisenberg A. Science 1995;268:1728–31.
(b) Petrov P, Rangelov S, Novakov Ch, Brown W, Berlinova I, Tsvetanov ChB. Polymer 2002;43:6641–51.
(c) Nicol E, Niepceron F, Bonnans-Plaisance C, Durand D. Polymer 2005;46:2020–8.
[6] Smulders W, Monteiro MJ. Macromolecules 2004;37:1174–4483.
[7] Castelvetro V, De Vita C. Adv Colloid Interface Sci 2004;108–109: 167–85.
[8] Ming W, Jones FN, Fu S. Macromol Chem Phys 1998;199:1075–9.
[9] Zhang Q, Remsen EE, Wooley KL. J Am Chem Soc 2000;122:3642–51.
[10] Liu S, Armes SP. J Am Chem Soc 2001;123:9910–1.
[11] Dou H, Jiang M, Peng H, Chen D, Hong Y. Angew Chem Int Ed 2003;42: 1516–9.
[12] (a) Hu Y, Jiang X, Ding Y, Ge H, Yuan Y, Yang C. Biomaterials 2003; 23:3193–201.
(b) Hu Y, Jiang X, Ding Y, Chen Q, Yang C. Adv Mater 2004;16(11): 933–7.
[13] (a) Cristallini C, Barbani N, Giusti P, Lazzeri L, Cascone MG, Ciardelli G. Macromol Chem Phys 2001;202:2104–13.
(b) Chauvierre C, Labarre D, Couvreur P, Vauthier C. Macromolecules 2003;36:6018–27.
[14] (a) Tauer K, Müller H, Schellenberg C, Rosengarten L. Colloids Surf, A: Physiochemical Eng Aspects 1999;153:143–51.
(b) Topp MDC, Leunen IH, Dijkstra PJ, Tauer K, Schellenberg C, Feijen J. Macromolecules 2000;33:4986–8.
(c) Athawale VD, Lele V. Carbohydrate Polym 2000;41:407–16.
[15] (a) Nurkeeva ZS, Mun GA, Khutoryanskiy VV. Macromol Biosci 2003; 3:283–95.
(b) Khutoryanskiy VV, Mun GA, Nurkeeva ZS, Dubolazov AV. Polym Int 2004;53:1382–7.
[16] Ryu J-G, Jeong Y-Il, Kim IHS, Lee J-H, Neh J-W, Kim S-H, Int J Pharm 2000;200:231–42.
[17] Burugapalli K, Bhatia D, Koul V, Choudhary V. J Appl Polym Sci 2001; 82:217–27.
[18] Burugapalli K, Koul V, Dinda AK. J Biomed Mater Res, Part A 2004; 68A:210–8.
[19] Ahn JS, Choi HK, Cho CS. Biomaterials 2001;22:923–8.
[20] Peniche C, Arguelles-Monal W, Davidenko N, Sastre R, Gallardo A, Roman JS. Biomaterials 1999;20:1869–78.
[21] Fyfe CA, McKinnon MS. Macromolecules 1986;19:1909–12.
[22] Carrot G, Valmalette JC, Plummer CJG, Scholz SM, Dutta J, Hofmann H, et al. Colloid Polym Sci 1998;276(10):853–9.
[23] Föster S, Plantenberg T. Angew Chem Int Ed 2002;41:688–714.
[24] (a) Zhang Y, Jiang M, Zhao J, Zhou J, Chen D. Macromolecules 2004;37: 1537–43.
(b) Ding Y, Hu Y, Jiang X, Zhang L, Yang C. Angew Chem Int Ed 2004; 43:6369–72.